ASSESSING PHYTOPLANKTON SIZE CLASSES FROM SATELLITE IN A COASTAL REGION OF THE SOUTH BRAZIL BIGHT

Andréa de Lima Oliveira[1], Natália Rudorff[2], Shubha Sathyendranath[3], Fábio Dall Cortivo[4] and Milton Kampel[5]

[1] National Institute For Space Research (INPE), Av. dos Astronautas, 1758 - Jardim da Granja, São José dos Campos - SP, 12227-010, andrea.oliveira@inpe.br,[2] INPE, natalia.rudorff@inpe.br, [3] Plymouth Marine Laboratory, Prospect Pl, Plymouth PL1 3DH, United Kingdom, ssat@pml.ac.uk,[4] INPE, fabio.cortivo@inpe.br, [5] INPE, milton.kampel@inpe.br

ABSTRACT

We used in situ phytoplankton diagnostic pigments to fit an algorithm to retrieve Phytoplankton Size Classes (PSCs) from chlorophyll-a. This regional algorithm was then applied to satellite data to analyze the seasonal and spatial variability of PSCs in the South Brazil Bight (SBB). Our results showed that this method could be an important tool for understanding the ecological dynamic of the SBB, and that the algorithm should be improved further.

Key words – *phytoplankton size classes, ocean color, diagnostic pigments, MODIS.*

1. INTRODUCTION

In the last two decades, several approaches were proposed to retrieve remote sensing estimations of phytoplankton size classes (PSCs) [1–4]. These algorithms have been tested both globally and locally, including coastal and continental shelf waters [5–8]. Regional algorithms are used to retrieve PSCs and to study their role in the oceanic carbon cycle, which is receiving a lot of attention and highlighting the need to understand long-term regional variability [9, 10]. Coastal waters are also relevant for human activities, such as leisure activities and are an important source of food (through fishing and marine aquaculture). Nonetheless, the coastal ecosystems are also highly sensitive to changing environmental conditions, driven by ocean acidification, sea level and temperature rise [11], which could intensify, for instance, the increase in algal bloom events [12], lead to reduction in the fishing stocks or in depletion of ideal conditions for cultivated species. In this study, we propose to answer the following research question: Does the abundance-based approach used to estimate PSCs perform well in this particular subtropical area? To this end we: (a) parameterize and evaluate the results of the abundance-based approach used to estimate PSC according to Brewin et al. (2010) when applied to a subtropical coastal area in the South Brazil Bright (SBB), (b) use the model to identify the dominant size class, by applying it to chlorophyll-*a* concentration derived from satellite data (Moderate Resolution Imaging Spectroradiometer - MODIS-Aqua imagery) processed with the Generalized Inherent Optical Properties framework with Default Configuration (GIOP-DC).

2. MATERIALS AND METHODS

The study area is located in the SBB, and is delimited in the north by Cabo Frio and in the south by the Cabo de Santa Marta (Figure 1). The sampling station was located around the isobath of 40m (varying from 42 to 44 m depending on the tide) in front of Ubatuba. The sampling period was from July 2006 to July 2019. From 2006 to 2015 the station was sampled monthly, and from 2016 on it was less frequently sampled, varying from 3 to 6 month interval between campaigns.

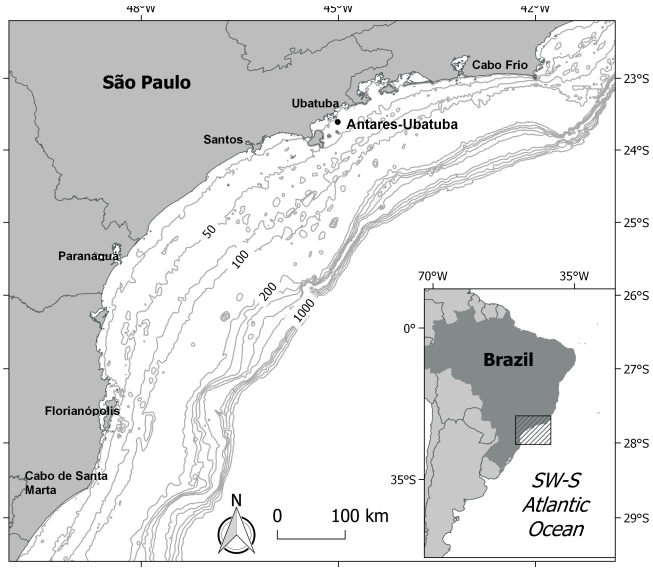


Figure 1: Antares-Ubatuba fixed time-series station (black circle) located in the inner shelf of the South Brazil Bight, limited by Cabo Frio in the North of the map and by Cabo de Santa Marta in the South. The bathymetry is represented by the gray lines.

2.1. Phytoplankton diagnostic pigments analysis

The phytoplankton diagnostic pigment concentrations were determined by High Performance Liquid Chromatography (HPLC). The samples were collected during 41 campaigns between July 2012 and May 2017. Surface water samples (1 m) were collected with a Niskin bottle, and 1 L of sample was filtered through glass fiber filters (0.7 μm) GF/F (Whatman®). Filters were stored and transported to the laboratory in liquid nitrogen and then maintained in an ultra-freezer at -80°C. All the samples were sent for pigment analysis using the HPLC method [13] at the NASA Goddard Space Flight Center, following well-established quality-control protocols. These pigments were used to estimate the fractions of each PSC using Diagnostic Pigment Analysis (DPA) [4] following Equation 1:

$$C = \sum_{i=1}^{7} W_i \cdot P_i \quad (1)$$

where C is the chlorophyll-*a* concentration estimated as the weighted sum of the diagnostic pigments, W_i is the weight attributed to each pigment i with a regional adjustment estimated in a previous study [14], and P_i is the concentration of diagnostic pigment. The pigments are given in this sequence: (1) Fucoxanthin, (2) Peridinin, (3) 19'-hexanoyloxyfucoxanthin, (4) 19'-butanoyloxyfucoxanthin, (5) Alloxanthin, (6) Total Chlorophyll-*b*, and (7) Zeaxanthin.

The fractions (F) for each size class considered here were estimated for the micro and nanophytoplankton ($F_{n,m}$) (Equation 2) considered together since it was indicated in a previous work in the region that the micro and nanophytoplankton would be difficult to distinguish by the pigment analysis [14]. And for the picophytoplankton (F_p) (Equation 3).

$$F_{n,m} = \frac{\sum_{i=1}^{5} W_i \cdot P_i}{C} \quad (2)$$

$$F_p = \frac{\sum_{i=6}^{7} W_i \cdot P_i}{C} \quad (3)$$

2.2. Model Parametrization of Phytoplankton Size Classes

Equations 2-3 were then multiplied by the measured Total Chlorophyll-*a* concentration (Chl*a*) to estimate chlorophyll associated to size class, and used as input to parameterize the model of Brewin et al. [1]. The chlorophyll-*a* concentrations of the picophytoplankton (C_p), combined nanophytoplankton and microphytoplankton ($C_{n,m}$), and the Chl*a*, measured by the HPLC analysis were fitted to the Equation 4 using a standard non-linear least-square fitting procedure (Levenberg-Marquardt). The fitting was performed with log-transformed Chl*a* values:

$$C_p = C_p^{max} \cdot [1 - exp(-S_p \cdot Chla)] \quad (4)$$

where C_p^{max} is the chlorophyll-*a* asymptotic maximum associated with the picophytoplankton, S_p is the initial slope for picophytoplankton. The estimated C_p is then used to estimate the $C_{m,n}$ using the following equation:

$$C_{n,m} = Chla - C_p \quad (5)$$

2.3. Satellite estimations

For satellite application, NASA MODIS-A level 1A images were downloaded and processed using SEADAS v8.1 to level 3, with 1.1 km spatial resolution, applying the GIOP-DC [15] and retrieving the satellite estimated chlorophyll-*a* concentration (Chla_{SAT}) and the Inherent Optical Properties (IOPs). The Chla_{SAT} values were then used to estimate the PSC fractions with the regionally-adjusted, abundance-based PSC algorithm.

2.4. Statistical metrics

The statistical metrics applied to compare the estimated values by the models and the in situ measured values were the correlation coefficient (ρ), root-mean-square error (RMSE), mean absolute error (MAE), and bias [16]. When the metrics were applied to Chl*a* data the $\log_{10}$ transformation was used, considering the known $log10$ distribution of Chl*a* [17]. Following Seegers et al. (2018) [16], we re-transformed the bias and MAE from the log10.

3. RESULTS AND DISCUSSION

3.1. Model Parametrization of Phytoplankton Size Classes

The modelled values of chlorophyll-*a* concentrations in each of the size classes and the fractions of the regionally adjusted abundance-based algorithm agreed reasonably well with the diagnostic pigment data (see Table 1 and Figure 2). The correlation coefficient varied from 0.63 to 0.94, and the bias indicated an overestimation of around 2% for the C_p and $F_{m,n}$ and of 12% for the $C_{m,n}$. The stations where algal bloom were present, i.e., with Chl*a* five times higher than the average value, the algorithm underestimated the picophytoplankton Chl*a*, since it reached the upper Chl*a* limit of this size fraction in the algorithm (C_p^{max}) (Figure 2).

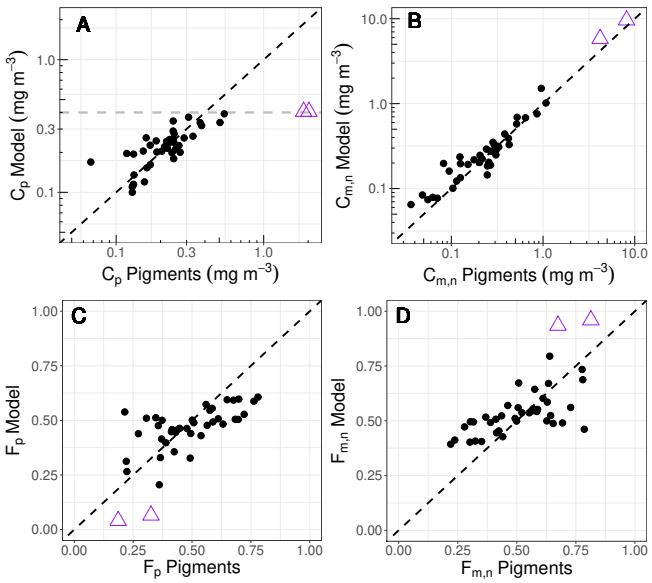


Figure 2: Scatter plots of the modelled values versus the diagnostic pigment analysis of chlorophyll-*a* concentration (A and B) and fractions for each size class (C and D). Dashed gray line in A is the C_p^{max}, the purple triangles are the algal bloom events. Dashed black line is the 1:1.

Variable	ρ	MAE	RMSE	Bias
C_p	0.76*	1.23	0.11	1.02
$C_{m,n}$	0.94*	1.26	0.13	1.12
$F_{m,n}$	0.63*	0.09	0.02	0.02

Table 1: Performance considering the modelled values and the values estimated with the pigments. (*) represent significance of p-value<0.01.

We observe that the initial slope for picophytoplankton (S_p) was relatively low (1.72) compared with other regions (Table 2). The S_p for other regions varied from 3.6 in the Northeast U.S. continental shelf [8] to 8.94 in the Southern Africa region [18]. The values for the C_p^{max} were less

variable, but the value was higher (0.40) compared with other studies, in which it varied from 0.11 for the global ocean [1] and Southern Africa [18] to 0.26 for Chinese coastal waters (West Pacific) [19]. Another parameter that is derived is D, which is the product of S_p and C_p^{max} and should be close to 1. The D value of this study (0.69) was at the lower end of previously reported values, which range from 0.54 to 1 (Table 2).

Region	S_p	C^p_{max}	D
SBB (This study)	1.72	0.40	0.69
Atlantic Ocean [1]	6.80	0.11	0.74
NOMAD [20]	5.12	0.15	0.77
West Pacific, coast [19]	3.85	0.26	1
Southern Africa, coastal [18]	8.94	0.11	0.98
Northeast U.S. continental shelf [8]	3.6	0.15	0.54

Table 2: Comparison of the PSC model's parameters from this study and in other regions.

Liu et al. (2018) [21] reported that picophytoplankton fraction presented a poor performance for all the models tested in the northwest Atlantic. The authors suggested that it could be related to the under-representation of pico-dominated samples in productive waters. However, this is not necessarily the case in the Antares-Ubatuba region, which does have an important fraction of picophytoplankton [14], but a low variability in the fractions sampled in the time series. One limitation of our study is the underrepresentation of the spatial distribution of the phytoplankton groups in relation to Chl*a* which underpins the algorithm applied here to the satellite data. Future work should seek to validate the approach used here, using data collected more broadly in the entire SBB. Of course, the time series nature of the data used here offers the possibility that the data collected over time would be representative of the different conditions prevalent in the area. But to improve that possibility, it would also be essential to increase the temporal resolution of sampling. Representative sampling is important, since the abundance-based algorithm applied here assumes that the relation between abundance (Chl*a*) and the phytoplankton size classes is fixed or stable, and does not account for changes in this relation.

3.2. Spatial and seasonal variability

Before applying abundance-based PSC to the Chla_{SAT} retrieved using the GIOP-DC applied to MODIS data, a validation exercise with the in situ Chl*a* was performed. The correlation coefficient was high, at 0.78; however, the bias indicated an overestimation of around 128% (N=23, including chlorophyll-*a* by measured by fluorometric method). Our station is very close to the shore and accurate satellite retrievals of remote sensing reflectance and IOPs are challenging due to adjacency effects, atmospheric correction and optical spectral mixture of in-water substances [22], and also because of a potential more complex assemblage of phytoplankton in coastal waters [23].

To reduce the $Chla_{SAT}$ bias we applied an adjustment to the in situ Chl*a*, by fitting a log-transformed linear regression between the Chl*a* (in situ) and the $Chla_{SAT}$, and the coefficients were used as follows in the Equation 6, where $Chla_{SAT\ <corr>}$ is the corrected value, and $Chla_{SAT}$ is the chlorophyll initially estimated from satellite.

$$Chla_{SAT\ <corr>} = 10^{(-0.3458\ +\ 0.6069\ \cdot\ log_{10}(Chla_{SAT}))} \quad (6)$$

The $Chla_{SAT\ <corr>}$ was used to estimate the $F_{m,n}$ for the seasonal means from 2002-2020 (Figure 3). Considering the SBB, the minimum in $F_{m,n}$ of 0.3 was observed at the shelf-break, with depths greater than 200m. These low values were observed during the austral summer (Figure 3A). The inner portion of the continental shelf presented higher values during all the seasons (at 50m isobath). During winter slightly high $F_{m,n}$ values were observed at the mid-shelf, with depths greater than 50m. This was not observed in other seasons.

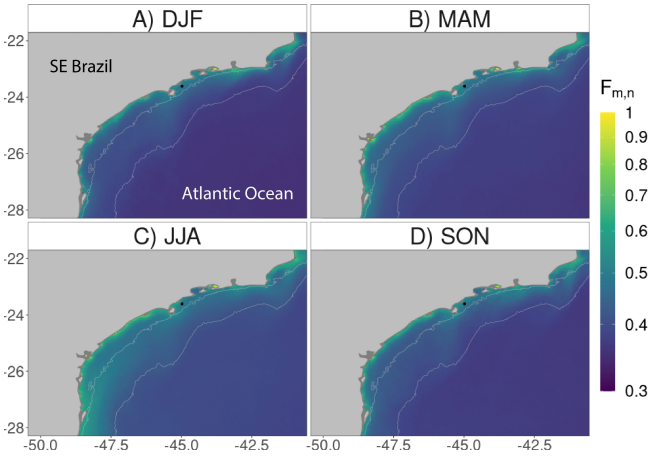


Figure 3: Seasonal average for the satellite estimated $F_{m,n}$, from 2002-2020, MODIS-Aqua. The letter up the figures are the months for the austral seasons: A) DJF (Dec, Jan and Feb) summer; B) MAM (Mar, Apr and May) autumn; C) JJA (Jun, Jul and Aug) winter; D) SON (Sep, Oct and Nov) spring. The gray lines are the isobaths of 50m (inner) and 200m (external). The black circle is the location of Antares-Ubatuba station.

4. CONCLUSIONS

To the best of our knowledge the work presented here represents the first attempt at a regional adjustment of abundance-based algorithms for retrieval of PSC in the SBB. Our results showed that the satellite retrieval PSC can enhance our understanding of the ecological dynamics in the region. However, for better retrievals, a regional PSC algorithm, which considers spatially-distributed in situ data and time series data at higher temporal resolution, is essential. In addition, the increasing number of space-borne hyperspectral radiometers that are now becoming available holds the potential to improve retrieval of phytoplankton size classes and phytoplankton functional types from space and present an opportunity for further development of this field.

5. ACKNOWLEDGMENTS

The Antares-Ubatuba time-series station is supported by the Oceanographic Institute of the University of São Paulo (IO-USP) and the National Institute for Space Research (INPE), Brazil, with contributions from other national and

international research agencies. We thank to all collaborators in the field work. ALO was supported by CAPES – Brazil (Grant Finance Code 001, 88882.330699/2019-01 and 88883.568456/2020-00). FDC was supported by a FUSP fellowship (N. 899, 2017/00686-0). MK acknowledges grants from FAPESP (2021/04128-8) and FUSP (2017/00686-0). We are also grateful for the access of the dataset from NASA Goddard Space Flight Center, Ocean Ecology Laboratory, Ocean Biology Processing Group; (2002 and 2020) for the MODIS-Aqua Imagery.

6. REFERENCES

[1] R. J W Brewin, S. Sathyendranath, T. Hirata, S. J Lavender, R. M. Barciela, and N. J. Hardman-mountford. A three-component model of phytoplankton size class for the Atlantic Ocean. *Ecological Modelling*, 221(11):1472–1483, 2010.

[2] E. Devred, S. Sathyendranath, V. Stuart, and T. Platt. A three component classification of phytoplankton absorption spectra : application to ocean color data. *Remote Sensing of Environment*, 115(9):2255–2266, 2011.

[3] S. Sathyendranath, G. Cota, V. Stuart, H. Maass, and T. Platt. Remote sensing of phytoplankton pigments: A comparison of empirical and theoretical approaches. *International Journal of Remote Sensing*, 22(2-3):249–273, 2001.

[4] J. Uitz, H. Claustre, A. Morel, and S. B. Hooker. Vertical distribution of phytoplankton communities in open ocean: an assessment based on surface chlorophyll. *Journal of Geophysical Research: Oceans*, 2006.

[5] B. Liu, E. J. D'Sa, K. Maiti, V. H. Rivera-Monroy, and Z. Xue. Biogeographical trends in phytoplankton community size structure using adaptive sentinel 3-OLCI chlorophyll a and spectral empirical orthogonal functions in the estuarine-shelf waters of the northern Gulf of Mexico. *Remote Sensing of Environment*, 252:112154, 2021.

[6] J.A. Gittings, R. J.W. Brewin, D. E. Raitsos, M. Kheireddine, M. Ouhssain, B. H. Jones, and I. Hoteit. Remotely sensing phytoplankton size structure in the Red Sea. *Remote Sensing of Environment*, 234:111387, 2019.

[7] D. Sun, Y. Huan, S. Wang, Z. Qiu, Z. Ling, Z. Mao, and Y. He. Remote sensing of spatial and temporal patterns of phytoplankton assemblages in the Bohai Sea, Yellow Sea, and east China sea. *Water Research*, 157:119–133, 2019.

[8] K. J. Turner, C. B. Mouw, K. J.W. Hyde, R. Morse, and A. B. Ciochetto. Optimization and assessment of phytoplankton size class algorithms for ocean color data on the Northeast U.S. continental shelf. *Remote Sensing of Environment*, 267:112729, 2021.

[9] A. Bracher, H. A. Bouman, R. J. W. Brewin, A. Bricaud, V. Brotas, A. M Ciotti, L. Clementson, and E. Devred. Obtaining phytoplankton diversity from ocean color : a scientific roadmap for future development. *Frontiers in Marine Science*, 4:1–15, 2017.

[10] R. J.W. Brewin, S. Sathyendranath, T. Platt, H. Bouman, and et al. Sensing the ocean biological carbon pump from space: a review of capabilities, concepts, research gaps and future developments. *Earth-Science Reviews*, 217:103604, 2021.

[11] B. Fox-Kemper, H. Hewitt, C. Xiao, and et al. Ocean, cryosphere and sea level change. In V. Masson-Delmotte, P. Zhai, A. Pirani, and et al., editors, *Climate change 2021: the physical science basis. contribution of working group I to the sixth assessment report of the intergovernmental panel on climate change science basis*, volume 2018, pages 1–257. Cambridge University Press, Cambridge, 2021.

[12] INTERGOVERNMENTAL PANEL ON CLIMATE CHANGE (IPCC). Summary for policymakers. In H.-O. Portner, D.C. Roberts, V. Masson-Delmotte, P. Zhai, M. Tignor, E. Poloczanska, K. Mintenbeck, A. Alegria, M. Nicolai, A. Okem, J. Petzold, B. Rama, and N.M. Weyer, editors, *IPCC special report on the ocean and cryosphere in a changing climate*. In press, 2019.

[13] L. VanHeukelem and S. B. Hooker. The importance of a quality assurance plan for method validation and minimizing uncertainties in the HPLC analysis of phytoplankton pigments. In S. Roy, C. A. Llewellyn, and E. S. Egeland, editors, *Phytoplankton Ppgments: characterization. chemotaxonomy and applications in oceanography*, pages 195–242. Cambridge University Press, Cambridge, 2011.

[14] A.L. Oliveira, N. Rudorff, M. Kampel, S. Sathyendranath, M. Pompeu, A. M. S. Detoni, and G. M. Cesar. Phytoplankton assemblages and optical properties in a coastal region of the South Brazil Bight. *Continental Shelf Research*, 227(June), 2021.

[15] P. J. Werdell, B. A. Franz, S. W. Bailey, G. C. Feldman, E. Boss, V. E. Brando, M. Dowell, T. Hirata, S. J. Lavender, Z. Lee, H. Loisel, S. Maritorena, F. Mélin, T. S. Moore, T. J. Smyth, D. Antoine, E. Devred, O. H. F. D'Andon, and A. Mangin. Generalized ocean color inversion model for retrieving marine inherent optical properties. *Applied Optics*, 52(10):2019, 2013.

[16] B. N. Seegers, R. P. Stumpf, B. A. Schaeffer, K. A. Loftin, and P. J.y Werdell. Performance metrics for the assessment of satellite data products: an ocean color case study. *Optics Express*, 26(6):7404, 2018.

[17] J. W. Campbell. The lognormal distribution as a model for bio-optical variability in the sea. *Journal of Geophysical Research*, 100(C7), 1995.

[18] T. Lamont, R. J. W. Brewin, and R. G. Barlow. Seasonal variation in remotely-sensed phytoplankton size structure around southern Africa. *Remote Sensing of Environment*, 204:617–631, 2018.

[19] Y. Huan, D. Sun, S. Wang, H. Zhang, Z. Qiu, M. Bilal, and Y. He. Remote sensing estimation of phytoplankton absorption associated with size classes in coastal waters. *Ecological Indicators*, 121:107198, 2021.

[20] R. J.W. Brewin, N. J. Hardman-Mountford, S. J. Lavender, D. E. Raitsos, T. Hirata, J. Uitz, E. Devred, A. Bricaud, A. Ciotti, and B. Gentili. An intercomparison of bio-optical techniques for detecting dominant phytoplankton size class from satellite remote sensing. *Remote Sensing of Environment*, 115(2):325–339, 2011.

[21] X. Liu, E. Devred, and C. Johnson. Remote sensing of phytoplankton size class in northwest Atlantic from 1998 to 2016: Bio-optical algorithms comparison and application. *Remote Sensing*, 10(7):1–25, 2018.

[22] INTERNATIONAL OCEAN-COLOUR COORDINATING GROUP (IOCCG). *Remote sensing of ocean colour in coastal, and other optically-complex, waters edited*, volume 3. IOCCG, Dartmouth, Canada, 2000.

[23] A. L. Oliveira, M. Kampel, N. Rudorff, and S Sathyendranath. The challenges of fitting phytoplankton size classes models to complex waters. In *Living Planet Symposium*, Bonn, 2022.